A new model for calculating the elastic local buckling stress of steel plates in square CFST columns

Yue-Ling Long [a,*], Lin Zeng [b], Leroy Gardner [c,*], M. Ahmer Wadee [c]

a. Department of Civil Engineering, Guangdong University of Technology, Guangzhou 510006, China.

b. Guangxi Vocational and Technical College of Communications, Nanning 530023, China.

c. Department of Civil and Environmental Engineering, Imperial College London, London SW7 2AZ, UK

*Corresponding authors: Yue-Ling Long(longyl@gdut.edu.cn)

and Leroy Gardner (leroy.gardner@imperial.ac.uk)

Abstract: Previous studies into the elastic local buckling response of the steel plates in concrete-filled steel tubular (CFST) sections have considered the effect of concrete infill on the plate boundary conditions and on the buckling mode shape (i.e. one-way buckling only), but have not considered the influence of hoop stresses. This is addressed in the current paper, where a new model is proposed in which the unloaded plate edges are assumed to be elastically restrained and account is taken of the influence of hoop stresses. Tensile hoop stresses are shown to delay the occurrence of local buckling in the steel plates of square and rectangular CFST sections, though their beneficial influence reduces with increasing rotational edge restraint. The model is verified against existing experimental results, revealing better predictions of elastic local buckling stresses compared to previous approaches. The influence of the key parameters — tensile hoop stresses, varying boundary conditions and differing width-to-thickness (b/t) ratios is subsequently explored using the developed model, where it is shown that the b/t ratio remains the dominant factor in defining the elastic local buckling stress of steel plates in CFST sections. Finally, an alternative equivalent thickness approach to allow for the influence of the hoop stresses is proposed.

Key words: Concrete-filled steel tubes; Hoop stresses; Local buckling; Plate buckling; Cross-section instability

1. Introduction

Concrete-filled steel tubular (CFST) columns have high strength, high ductility and excellent energy absorption capacity due to the composite effects of the steel tube and infilled concrete, resulting in extensive applications in building and bridge structures [1-6]. In recent years, there has been a keen interest in evaluating the local buckling behaviour of CFST columns, aimed at developing a full understanding of the interaction between the two components and hence exploiting the composite action to the greatest extent. A number of relevant studies have been conducted on both circular and square/rectangular CFST columns including those by Ge et al. [7-8], Wright [9-10], Bradford et al. [11-12], Uy et al. [13-15], Liang et al. [16-19] and Long et al. [20-22]. Based on these studies, it has been concluded that the steel plates in CFST columns subjected to axial compression can only buckle outwards due to presence of the infilled concrete and that local buckling of the steel plates, particularly in the case of square/rectangular CFST columns, plays a key role in their design.

It has been shown in previous experimental and analytical studies that tensile hoop stresses develop in the steel tube of square and rectangular CFST columns subjected to axial compression, which increase until the steel tube buckles locally [1-2]. However, these hoop stresses are ignored in all existing models concerning local buckling of the steel plates in square and rectangular CFST columns, which could explain the differences previously observed between predicted and experimentally-obtained results, especially for cross-sections subjected to combined loading. In order to advance the understanding of the influence of the hoop stresses on the local buckling behavior of square CFST columns, a new model is developed herein. The model is verified against experimental results and is subsequently employed to investigate the influence of tensile hoop stresses, boundary conditions and width-to-thickness ratios on the elastic local buckling of the steel plates in square CFST columns. The influence of the key model parameters on the elastic local buckling stress is discussed in detail. Finally, a unified equation for predicting the elastic local buckling stress of steel plates, allowing for the influence of hoop stresses and featuring an equivalent plate thickness, is proposed.

2. Overview of existing models

Existing models to predict the local buckling behaviour of steel plates in square CFST columns are indicated in Fig. 1(a), (b) and (c). As shown in Fig. 1, the loaded edges of the steel plate in square CFST columns are assumed to be clamped in all existing models. The unloaded edges of the steel plate are respectively assumed to be simply-supported (see Fig. 1(a)),

clamped (see Fig. 1(b)) and elastically restrained against rotation (see Fig. 1(c)) in the different models. All these models were devised using energy methods. Based on the models shown in Fig. 1(a), Fig. 1(b) and Fig. 1(c), the derived elastic local buckling stresses of the steel plates are expressed respectively in Eq. (1), Eq. (2) and Eq. (3).

$$\sigma_{cr} = 5.46\frac{\pi^2 E}{12(1-v^2)(b/t)^2} \tag{1}$$

$$\sigma_{cr} = 10.31\frac{\pi^2 E}{12(1-v^2)(b/t)^2} \tag{2}$$

$$\sigma_{cr} = \left\{\frac{\sqrt{3A_2+6\chi\ (1+A_5^{\ 2})}}{\pi^2\sqrt{A_1}} + \frac{2(1-v)A_3-2A_4}{\pi^2 A_1} + \frac{3A_2+6\chi(1+A_5^{\ 2})}{\pi^2\sqrt{A_1[3A_2+6\chi(1+A_5^{\ 2})]}}\right\}\times\frac{\pi^2 E}{12(1-v^2)(b/t)^2} \tag{3}$$

where E is elastic modulus of the steel plates, v is Poisson's ratio of the steel plates, χ is the elastic restraining factor, b and t are respectively the width and thickness of the steel plates, while A_1, A_2, A_3, A_4 and A_5 are detailed in the Appendix. It was shown in [20] that the elastic buckling stresses calculated using Eqs. (1) and (2) provide a lower and upper bound respectively to test results, while more accurate predictions are achieved with the intermediate boundary conditions assumed in Eq.(3) and shown in Fig. 1(c). However, inconsistencies in the predictions remain and these are attributed to the simplifying assumptions of ignoring the influence of hoop stresses. The suitability of this simplifying assumption is carefully studied in the present paper.

3. New model for local buckling of steel plates in square CFST sections incorporating the influence of tensile hoop stresses

A new model for determining the elastic local buckling stress of the steel plates in square CFST columns is proposed, in which the influence of tensile hoop stresses is considered. For the sake of simplicity, the tensile hoop stresses in the steel plates are assumed to be uniformly distributed, as shown in Fig. 2. In addition, it is assumed that the unloaded edges are elastically restrained against rotation while the loaded edges are assumed to be clamped in line with previous research (see Fig. 2).

3.1 Potential energy model

Based on the theory of elastic stability [24], the governing partial differential equation for the critical buckling of a thin plate is expressed as:

$$D\left(\frac{\partial^4 \omega}{\partial x^4} + 2\frac{\partial^4 \omega}{\partial x^2 \partial y^2} + \frac{\partial^4 \omega}{\partial y^4}\right) = N_x \frac{\partial^2 \omega}{\partial x^2} + 2N_{xy}\frac{\partial^2 \omega}{\partial x \partial y} + N_y \frac{\partial^2 \omega}{\partial y^2} \tag{4}$$

where t and v respectively are thickness and Poisson's ratio of the steel plate, ω is the deflection function, N_x and N_y are normal forces per unit length in x and y directions, respectively, N_{xy} is shear force per unit length in the xy-plane and D is the flexural rigidity of the plate, given by:

$$D = \frac{Et^3}{12(1-v^2)} \tag{5}$$

Similarly, the strain energy associated with thin plate bending U and the work done by the applied loading V are expressed by Eqs. (6) and (7), respectively.

$$U = \frac{D}{2}\iint\left\{\left(\frac{\partial^2 \omega}{\partial x^2}\right)^2 + 2\frac{\partial^2 \omega}{\partial x^2}\frac{\partial^2 \omega}{\partial y^2} + \left(\frac{\partial^2 \omega}{\partial y^2}\right)^2 - 2(1-v)\left[\frac{\partial^2 \omega}{\partial x^2}\frac{\partial^2 \omega}{\partial y^2} - \left(\frac{\partial^2 \omega}{\partial x \partial y}\right)^2\right]\right\}dxdy \tag{6}$$

$$V = \frac{1}{2}\iint\left[N_x\left(\frac{\partial \omega}{\partial x}\right)^2 + 2N_{xy}\left(\frac{\partial \omega}{\partial x}\frac{\partial \omega}{\partial y}\right) + N_y\left(\frac{\partial \omega}{\partial y}\right)^2\right]dxdy \tag{7}$$

As indicated in Fig. 2, the applied boundary stresses acting on the steel plates in square CFST columns subjected to axial compression are:

$$N_x = -\sigma_x t \tag{8}$$

$$N_y = -\sigma_y t \tag{9}$$

$$N_{xy} = \tau_{xy} t = 0 \tag{10}$$

where σ_x is the uniform compressive stress in the x-axis direction and σ_y is the corresponding uniform tensile hoop stress

in the *y*-axis direction, indicated in Fig. 2.

The uniform tensile hoop stress σ_y can be also expressed thus:

$$\sigma_y = -m\sigma_x \qquad (m \geq 0) \tag{11}$$

where m is the ratio of tensile hoop stress σ_y to the compressive longitudinal stress σ_x. Substituting Eq. (11) into Eq. (9) results in:

$$N_y = -\sigma_y t = m\sigma_x t \tag{12}$$

Based on the research presented in [20], which assumed that the loaded edges of the steel plates in CFST columns are clamped and the unloaded edges are elastically restrained against rotation, the deformed shape can be expressed as:

$$\omega = c\left[\frac{y}{b} + \phi_1\left(\frac{y}{b}\right)^2 + \phi_2\left(\frac{y}{b}\right)^3 + \phi_3\left(\frac{y}{b}\right)^4\right]\left(1 - \cos\frac{2\pi x}{a}\right) \tag{13}$$

where a and b are the buckling half wavelength and width of the steel plate, respectively, c is a generalized coordinate that defines the amplitude of the deformed shape and ϕ_1, ϕ_2 and ϕ_3 are given by

$$\left.\begin{aligned} \phi_1 &= \chi \\ \phi_2 &= -2(\chi + 1) \\ \phi_3 &= \chi + 1 \end{aligned}\right\} \tag{14}$$

in which χ is the elastic restraining factor for the unloaded edges, given by

$$\chi = \frac{\zeta_r b}{2D} \tag{15}$$

where ζ_r is rotational rigidity of the elastic restraints along the unloaded edges.

The total potential energy of the plate Π can be expressed as

$$\Pi = U + V + U_\Gamma \tag{16}$$

where U and V where defined above and U_Γ is the strain energy associated with the elastic restraint along the unloaded edges, given by

$$U_\Gamma = \frac{\zeta_r}{2}\int_\Gamma \left[\left(\frac{\partial \omega}{\partial y}\right)^2_{y=0} + \left(\frac{\partial \omega}{\partial y}\right)^2_{y=b}\right] d\Gamma \tag{17}$$

Substituting Eqs. (6)- (14) and (17) into Eq. (16) results in

$$\Pi = \frac{D}{2}\left[\frac{8\pi^4 c^2 b}{a^3}A_1 - \frac{4\pi^2 c^2}{ab}A_4 + \frac{3ac^2}{2b^3}A_2 + 2(1-\nu)\frac{2\pi^2 c^2}{ab}A_3\right] + \frac{3c^2\zeta_r a(1+A_5^{\,2})}{4b^2} - \frac{\pi^2 c^2 b\sigma_x t}{a}A_1 + \frac{3mc^2 a\sigma_x t}{4b}A_6 \tag{18}$$

in which A_1-A_6 are given by

$$\left.\begin{aligned}
A_1 &= \frac{1}{3} + \frac{\phi_1}{2} + \frac{\phi_1^{\,2} + 2\phi_2}{5} + \frac{\phi_3 + \phi_1\phi_2}{3} + \frac{\phi_2^{\,2} + 2\phi_1\phi_3}{7} + \frac{\phi_2\phi_3}{4} + \frac{\phi_3^{\,2}}{9}\\
A_2 &= 4\phi_1^{\,2} + 12\phi_2^{\,2} + 12\phi_1\phi_2 + \frac{144}{5}\phi_3^{\,2} + 16\phi_1\phi_3 + 36\phi_2\phi_3\\
A_3 &= 1 + 3\phi_1 + 2\phi_1^{\,2} + 4\phi_2 + 5\phi_3 + 5\phi_1\phi_2 + 6\phi_1\phi_3 + 7\phi_2\phi_3 + 3\phi_2^{\,2} + 4\phi_3^{\,2}\\
A_4 &= \phi_1 + \frac{2\phi_1^{\,2} + 6\phi_2}{3} + 3\phi_3 + 2\phi_1\phi_2 + \frac{14\phi_1\phi_3 + 6\phi_2^{\,2}}{5} + 3\phi_2\phi_3 + \frac{12\phi_3^{\,2}}{7}\\
A_5 &= 1 + 2\phi_1 + 3\phi_2 + 4\phi_3\\
A_6 &= A_3 - A_4 = 1 + 2\phi_1 + 2\phi_2 + 2\phi_3 + \frac{4\phi_1^{\,2}}{3} + \frac{9\phi_2^{\,2}}{5} + \frac{16\phi_3^{\,2}}{7} + 3\phi_1\phi_2 + \frac{16\phi_1\phi_3}{5} + 4\phi_2\phi_3
\end{aligned}\right\} \tag{19}$$

The condition of stationary potential energy provides the equilibrium equation. This is determined by setting the partial derivative of the total potential energy with respect to the generalized coordinate c equal to zero, as given by:

$$\frac{\partial \Pi}{\partial c} = 0 \tag{20}$$

Hence, combining Eqs. (18) and (20) yields the following equilibrium equation.

$$\sigma_x t = \frac{\frac{16\pi^2}{\gamma^2}A_1 - 8A_4 + \frac{3\gamma^2}{\pi^2}A_2 + 8(1-\nu)A_3 + \frac{6\chi\gamma^2(1+A_5^{\,2})}{\pi^2}}{4\pi^2 A_1 - 3m\gamma^2 A_6}\frac{D\pi^2}{b^2} = k\frac{D\pi^2}{b^2} \tag{21}$$

where γ is the ratio of the longitudinal to the transverse local buckling half-wavelength, given by

$$\gamma = \frac{a}{b} \tag{22}$$

and k is the elastic local buckling coefficient, given by

$$k = \frac{\frac{16\pi^2}{\gamma^2}A_1 - 8A_4 + \frac{3\gamma^2}{\pi^2}A_2 + 8(1-\nu)A_3 + \frac{6\chi\gamma^2(1+A_5^{\,2})}{\pi^2}}{4\pi^2 A_1 - 3m\gamma^2 A_6} \tag{23}$$

Setting $\frac{\partial k}{\partial \gamma} = 0$ reveals the critical value of γ, denoted γ_{cr}, at which the minimum value of k arises, as given by:

$$\gamma_{cr}^{\ 2} = 4\pi^2 \frac{A_1\left[\sqrt{3A_1A_2 + 6\chi A_1(1 + A_5^{\ 2}) + 6(1 - \nu)mA_3A_6 - 6mA_4A_6 + 9m^2A_6^{\ 2}} - 3mA_6\right]}{3A_1A_2 + 6\chi A_1(1 + A_5^{\ 2}) + 6(1 - \nu)mA_3A_6 - 6mA_4A_6} \tag{24}$$

Substituting Eq. (24) into (23) yields the minimum value of the elastic local buckling coefficient k, denoted k_{cr} as given by:

$$\begin{aligned} k_{cr} = & \frac{6\left[A_2 + 2\chi\left(1 + A_5^{\ 2}\right)\right]}{\pi^2\left[\sqrt{3A_1A_2 + 6\chi A_1\left(1 + A_5^{\ 2}\right) + 6(1 - \nu)mA_3A_6 - 6mA_4A_6 + 9m^2A_6^{\ 2}} - 3mA_6\right]} \\ & + \frac{2\left[(1 - \nu)A_3 - A_4\right]\left[3A_1A_2 + 6\chi A_1\left(1 + A_5^{\ 2}\right) + 6(1 - \nu)mA_3A_6 - 6mA_4A_6\right]}{\pi^2A_1\left[\sqrt{3A_1A_2 + 6\chi A_1\left(1 + A_5^{\ 2}\right) + 6(1 - \nu)mA_3A_6 - 6mA_4A_6 + 9m^2A_6^{\ 2}} - 3mA_6\right]^2} \end{aligned} \tag{25}$$

Hence, the elastic local critical buckling stress of the steel plate is:

$$\begin{aligned} \sigma_{cr} = & \frac{\pi^2E}{12(1-\nu^2)(b/t)^2} \times \left\{ \frac{6\left[A_2 + 2\chi(1 + A_5^{\ 2})\right]}{\pi^2\left[\sqrt{3A_1A_2 + 6\chi A_1\left(1 + A_5^{\ 2}\right) + 6(1 - \nu)mA_3A_6 - 6mA_4A_6 + 9m^2A_6^{\ 2}} - 3mA_6\right]} \right. \\ & \left. + \frac{2\left[(1-\nu)A_3 - A_4\right]\left[3A_1A_2 + 6\chi A_1\left(1 + A_5^{\ 2}\right) + 6(1 - \nu)mA_3A_6 - 6mA_4A_6\right]}{\pi^2A_1\left[\sqrt{3A_1A_2 + 6\chi A_1\left(1 + A_5^{\ 2}\right) + 6(1 - \nu)mA_3A_6 - 6mA_4A_6 + 9m^2A_6^{\ 2}} - 3mA_6\right]^2} \right\} \end{aligned} \tag{26}$$

For the particular case of m=0 i.e. the case in which the influence of the tensile hoop stresses in the steel plate is ignored, Eq. (25) reduces to the following relationship:

$$k_{cr0} = \frac{\sqrt{3A_2 + 6\chi(1 + A_5^{\ 2})}}{\pi^2\sqrt{A_1}} + \frac{2(1-\nu)A_3 - 2A_4}{\pi^2A_1} + \frac{3A_2 + 6\chi(1 + A_5^{\ 2})}{\pi^2\sqrt{A_1[3A_2 + 6\chi(1 + A_5^{\ 2})]}} \tag{27}$$

which accords with the results presented in [22].

The corresponding elastic critical local buckling stress, for the case of m=0, is:

$$\sigma_{\mathrm{cr0}} = \frac{\pi^2 E}{12\left(1-\nu^2\right)(b/t)^2}\left\{\frac{\sqrt{3A_2+6\chi\left(1+A_5{}^2\right)}}{\pi^2\sqrt{A_1}}+\frac{2(1-\nu)A_3-2A_4}{\pi^2 A_1}+\frac{3A_2+6\chi\left(1+A_5{}^2\right)}{\pi^2\sqrt{A_1\left[3A_2+6\chi\left(1+A_5{}^2\right)\right]}}\right\} \tag{28}$$

which again corresponds with the results of previous studies [20, 22].

3.2 Discussion on model parameters

3.2.1 Influence of parameter m on plate critical stress

The influence of the ratios m and b/t on the elastic critical local buckling stress σ_{cr} for different boundary conditions is illustrated in Fig. 3. It can be observed that σ_{cr} increases with increasing values of m, indicating that the tensile hoop stresses delay the occurrence of local buckling. The influence of m on σ_{cr} is more significant for plates with smaller b/t ratios; hence, the influence of m on σ_{cr} can be neglected when b/t ratios are sufficiently large. In order to evaluate the influence of m on σ_{cr}, the parameter δ_{m}, defined by Eq. (29), is introduced.

$$\delta_{\mathrm{m}} = \frac{\sigma_{\mathrm{cr1}}-\sigma_{\mathrm{cr0}}}{\sigma_{\mathrm{cr0}}} \tag{29}$$

where σ_{cr0} is the elastic critical local buckling stress in the case of m=0 and σ_{cr1} is the elastic critical local buckling stress in the case of m>0.

According to the proposed model, the required values of m to achieve set values of δ_{m} for different boundary conditions are listed in Table 1. Similarly, Fig. 4 shows the relationship between δ_{m} and m for different values of the elastic restraining factor for the unloaded plate edges χ. As shown in Fig. 4 and Table 1, δ_{m} is strongly influenced by the boundary conditions along the unloaded plate edges. For a given value of m, δ_{m} is greater in the case of simply-supported

unloaded edges than in the case of clamped unloaded edges, implying that the influence of tensile hoop tresses on σ_{cr} reduces with increasing rotational edge restraint. In addition, δ_m increases with increasing values of m.

For a given value of χ, the relationship between δ_m and m can be approximately described by a straight line, as indicated in Fig. 4. The relationships between δ_m and m for the cases χ=0 and $\chi \rightarrow \infty$, as determined by linear regression, are given by Eq. (30) and Eq. (31), respectively and illustrated in Fig. 5.

$$\delta_m = 1.94m \qquad \text{for} \quad \chi=0 \tag{30}$$

$$\delta_m = 1.09m \qquad \text{for} \quad \chi \rightarrow \infty \tag{31}$$

It can be seen from Fig. 5 that the curves described by Eq. (30) and Eq. (31) are both in close agreement with the results calculated using the proposed analytical model. The differences between the curves and the results calculated using the proposed model are less than 1%. Hence, it is demonstrated that the relationship between δ_m and m at a specified value of χ can be closely approximated by a linear equation.

It should be noted that although the proposed model was developed with steel plates in CFST sections in mind, where the hoop stresses are tensile, it does, in fact, also apply in the case of compressive hoop stresses (i.e. m<0). Fig. 6 shows the influence of m on the relationship between σ_{cr} and b/t. It can be seen that the critical stress σ_{cr} decreases considerably with only a modest decrease in m when m<0 i.e. in the case of biaxial compression. Also, the influence of m on σ_{cr}, in the case of m>0, is more significant than in the case of m<0. Further analysis of the local buckling of steel plates with compressive hoop stresses will be carried out in future work.

3.2.2 Influence of elastic restraining factor on plate critical stress

Fig. 7 shows the influence of the elastic restraining factor for the unloaded edges χ on the elastic critical local buckling

coefficient k_{cr} for different values of m. It may be observed that k_{cr} increases as χ increases for a given value of m, and that k_{cr} also increases as m increases for a given value of χ. Furthermore, it is found that k_{cr} increases significantly with increasing χ when $\chi \leq 25$; when $\chi > 25$, the influence of χ on k_{cr} becomes weak and k_{cr} approaches a constant value when χ becomes large. Table 2 gives the values of k_{cr} with varying m for different boundary conditions along unloaded edges.

For steel plates with a given b/t ratio, the local critical buckling stress σ_{cr} increases with χ, but at a decreasing rate as $\chi \to \infty$, as shown in Fig. 8. The values of χ at which σ_{cr} differs by 5% from the case where $\chi \to \infty$ can be derived from the proposed model, and are denoted by an asterisk in the legends of the graphs, for different values of m, in Fig. 8. The determined values of χ lie between 30 and 35. Hence, it can be stated that the σ_{cr} - b/t curves for $\chi \geq 35$ and $\chi \to \infty$ are almost the same. Similarly, it can be seen that the σ_{cr} - b/t curves for $\chi \leq 0.2$ and $\chi = 0$ are almost the same. The corresponding k_{cr} values are also listed in Table 2 for the cases of $\chi = 35$ and $\chi = 0.2$. It can be seen from Fig. 8 (a)-(d) that the influence of χ on σ_{cr} weakens with increasing m. In particular, when $m \to \infty$, the curves with varying values of χ are almost the same, as illustrated in Fig. 8 (e) i.e. the influence of the boundary conditions on σ_{cr} diminishes as $m \to \infty$. Moreover, when $m \to \infty$, $k_{cr} \to \infty$, i.e. local buckling ceases to occur — a finding that corresponds with physical observations.

3.3 Qualitative analysis of different influence factors

It was shown in Section 3.2 that σ_{cr} is principally influenced by three factors, namely: the b/t ratio of the steel plate, m and χ, as indicated in Fig.9. Specimens S1-S5 were selected to investigate the influence of χ and m on σ_{cr} for different b/t ratios, as presented in Fig.10. By comparing specimens S2 and S4 with S1 (or specimens S3 and S5 with S1), it can be seen that the influence of m on σ_{cr} is more significant than the influence of χ, implying that increasing the tensile hoop stress is more effective than increasing the elastic restraining factor on the unloaded edges in enhancing the elastic

critical local buckling stress. Similarly, specimens S6-S10 were selected to assess the influence of the *b*/*t* ratio and *m* on σ_{cr}, as shown in Fig. 11. It can be observed that σ_{cr} is influenced by both the *b*/*t* ratio and *m*, with the influence of the *b*/*t* ratio being more significant than that of *m*; this can be seen by comparing specimens S7 and S9 with S6 (or specimens S8 and S10 with S6), which reveals that decreasing the *b*/*t* ratio is more effective than increasing the tensile hoop stresses in enhancing the elastic critical local buckling stress of steel plates.

Based on the above discussion, it can be concluded that σ_{cr} is most strongly influenced by the *b*/*t* ratio, then by *m*, and least by χ. Hence, decreasing the width-to-wall thickness ratio remains key to delaying the occurrence of local buckling in the steel plates of CFST cross-sections.

3.4 Determination of χ for square CFST columns

Based on previous research [20-22], the elastic restraining factor χ on the unloaded edges of steel plates in CFST sections can be determined from the following relationship:

$$\chi = \left(\frac{0.8 t_{\mathrm{w}}}{t_{\mathrm{f}}} \right)^3 \frac{r'}{\rho} \tag{32}$$

where

$$r' = 2 - \left(\frac{t_{\mathrm{f}} b_{\mathrm{w}}}{t_{\mathrm{w}} b_{\mathrm{f}}} \right)^2 \tag{33}$$

and

$$\rho = \frac{1}{\pi} \tanh\left(\frac{\pi b_{\mathrm{w}}}{4 b_{\mathrm{f}}} \right) \left[1 + \frac{\pi b_{\mathrm{w}} / 2 b_{\mathrm{f}}}{\sinh\left(\pi b_{\mathrm{w}} / 2 b_{\mathrm{f}} \right)} \right], \tag{34}$$

in which b_{f} and b_{w} are respectively the widths of the steel plate in question and that of the adjacent steel plate and t_{f} and t_{w} are respectively the thicknesses of the steel plate in question and that of the adjacent steel plate. For square CFST sections specially, substituting $t_{\mathrm{f}}=t_{\mathrm{w}}$ and $b_{\mathrm{f}}=b_{\mathrm{w}}$ into Eqs (32)-(34) reveals that the elastic restraining factor reduces to

simply χ=1.46; the corresponding relationship between δ_m and m in the case of χ=1.46 is also listed in Table 1.

3.5 Determination of m

The concept of effectively and ineffectively confined regions to describe the non-uniform confinement afforded to square/rectangular concrete blocks by square/rectangular steel hoops was proposed in [25]. This concept was extended in [26-27] to take account of the non-uniformity of concrete confinement in square/rectangular CFST columns with and without binding bars.

A similar approach is adopted herein to consider the non-uniformity of the tensile hoop stresses that arise within the steel plate of square CFST columns. Specifically, a reduction factor k_e is applied to the maximum value of the ratio of the tensile hoop stress to the compressive axial stress m_{max} (see below) in the steel plate of square CFST columns to provide an equivalent uniform value of m, hence:

$$m = k_e m_{max} \tag{35}$$

where m_{max} is taken as 0.21 for square CFT sections according to the findings of Sankino et. al [1].

According to Refs [26-27], k_e can be taken as:

$$k_e = \frac{A_1}{A} = \frac{A_1}{A_1 + A_2} = 1 - \frac{2\tan\theta}{3} \quad (\theta \le 45°) \tag{36}$$

where A is the cross-sectional area of the concrete core, A_1 and A_2 are respectively the cross-sectional areas of the effectively confined regions and the ineffectively confined regions of the concrete core and θ is the initial tangent angle discussed below. The effectively and ineffectively confined regions of the concrete are shown in Fig. 12. The ineffectively confined regions of the concrete are assumed to be the areas enclosed by a parabola with an initial tangent

angle θ.

Eq. (36) is only applicable to the case of $\theta \leq 45°$. When $\theta > 45°$, there are overlapping areas in the ineffectively confined regions of the confined concrete, which should be deducted, leading to the following expression.

$$k_e = \frac{A_1}{A} = \frac{A_1}{A_1 + A_2} = \frac{2\tan\theta}{3} + \frac{4}{\tan\theta} - \frac{4}{3\tan^2\theta} - 3 \quad (\theta > 45°) \tag{37}$$

Mander et.al [25] proposed the initial tangent angle θ=45° for square/rectangular reinforced concrete columns, though this was found to be inappropriate for square/rectangular CFST columns [26-27]. An empirical equation for θ for square CFST sections is proposed herein, in which θ is a function of the b/t ratio of the steel plate:

$$\theta = 15°\sin\left[\frac{(b/t)\pi}{120} + (b/t)\right] + 49.5° \tag{38}$$

As a simplification, for ease of application, a constant value of θ=57° may be assumed.

4. Assessment of accuracy of proposed model

In this section, the accuracy of the proposed model is assessed against a series of test results for the elastic critical local buckling stress $\sigma_{cr,\,test}$ of steel plates in square CFST columns collected from literature [12, 14], as presented in Table 3. The calculated local buckling stresses σ_{cr} using the proposed model are compared with those determined experimentally, as well as those calculated using other prediction models [9,10,16-18,20]. As shown in Table 3, the calculated results using the proposed model provide the closest agreement with the test results; this is attributed to the consideration of the influence of tensile hoop stresses on the local buckling stress of the steel plates in square CFST columns.

Comparisons are also made against the predictions of an existing empirical equation [17], given by Eq. (40), for determining the elastic critical local buckling stress of steel plates in CFST columns, applicable for b/t ratios between 30

and 100.

$$\frac{\sigma_{cr}}{f_y} = a_1 + a_2\left(\frac{b}{t}\right) + a_3\left(\frac{b}{t}\right)^2 + a_4\left(\frac{b}{t}\right)^3 \tag{40}$$

in which the coefficients a_1, a_2, a_3 and a_4 are detailed in Ref. [17]. A comparison between the results of the proposed model and those obtained from Eq. (40) is presented in Fig. 13, where reasonable agreement can be seen, particularly in the range where $b/t \geqslant 70$.

5. Equivalent thickness concept to consider influence of hoop stresses

An equivalent thickness concept to consider the influence of hoop stresses is proposed in this section. The proposed equivalent thickness t_{eq} is given by Eq. (41); the positive influence of tensile hoop stresses (such as those that arise in square CFST sections) is captured through an increase in plate thickness (i.e. $t_{eq}>t$), while the negative influence of compressive hoop stresses is captured through a reduction in plate thickness (i.e. $t_{eq}<t$).

.

$$t_{eq} = t\sqrt{\frac{k_{cr}}{k_{cr0}}} \tag{41}$$

where k_{cr} was given by Eq. (25) and k_{cr0} is the elastic critical local buckling coefficient that neglects the influence of hoop stresses, as given in Eq. (27).

The calculation of t_{eq}, as given by Eq. (41), can be simplified by observing (from Eqs. (25) and (27)) that, for the same boundary conditions, t_{eq} depends only on m. Hence, best-fit relationships between t_{eq} and m have been derived for the cases where the unloaded plate edges are simply-supported, elastically restrained against rotation and clamped, as given by Eqs. (42),(43) and (44), respectively.

$$t_{eq} = \begin{cases} \left(-3.06e^{\frac{-m}{3.7}} + 4.06\right)t & (m \geq 0) \\ \left(0.8e^{\frac{m}{0.7}} + 0.22\right)t & (m < 0) \end{cases}$$ for simply-supported edges (42)

$$t_{eq} = \begin{cases} \left(-3e^{\frac{-m}{4.6}} + 4\right)t & (m \geq 0) \\ \left(0.75e^{m} + 0.25\right)t & (m < 0) \end{cases}$$ for elastically restrained edges (43)

$$t_{eq} = \begin{cases} \left(-3.2e^{\frac{-m}{6.4}} + 4.2\right)t & (m \geq 0) \\ \left(0.7e^{\frac{m}{1.3}} + 0.3\right)t & (m < 0) \end{cases}$$ for clamped edges (44)

Figs. 14(a), (b) and (c) show that the predicted results determined using Eqs. (42)-(44) follow closely those calculated using Eq. (41), with a coefficient of variation of less than 5%. Hence, as an alternative to the use of Eq. (26), the elastic critical local buckling stress of steel plates in square CFST sections may be determined from Eq. (45), with k_{c0} from Eq.(27) and t_{eq} from Eqs. (42)-(44), depending on the boundary conditions.

$$\sigma_{cr} = \frac{k_{cr0}\pi^2 E}{12\left(1-\nu^2\right)}\left(\frac{t_{eq}}{b}\right)^2 \quad (45)$$

6. Summary

The elastic critical local buckling stress σ_{cr} of the steel plates in square CFST columns can be calculated, allowing for the influence of the *b/t* ratio as well as the restriction to the buckling mode shape and the tensile hoop stresses arising due to the presence of the concrete infill from:

$$\sigma_{cr} = \frac{k_{cr}\pi^2 E}{12(1-\nu^2)}\left(\frac{t}{b}\right)^2 \quad (46)$$

where

$$k_{cr} = \frac{6\left[A_2 + 2\chi\left(1 + A_5^{\,2}\right)\right]}{\pi^2\left[\sqrt{3A_1A_2 + 6\chi A_1\left(1 + A_5^{\,2}\right) + 6(1-\nu)mA_3A_6 - 6mA_4A_6 + 9m^2A_6^{\,2}} - 3mA_6\right]} + \frac{2\left[(1-\nu)A_3 - A_4\right]\left[3A_1A_2 + 6\chi A_1\left(1 + A_5^{\,2}\right) + 6(1-\nu)mA_3A_6 - 6mA_4A_6\right]}{\pi^2A_1\left[\sqrt{3A_1A_2 + 6\chi A_1\left(1 + A_5^{\,2}\right) + 6(1-\nu)mA_3A_6 - 6mA_4A_6 + 9m^2A_6^{\,2}} - 3mA_6\right]^2}.$$

Alternatively, σ_{cr} may be determine from Eq.(47), with the restriction to the buckling mode shape accounted for through k_{c0} and the tensile hoop stresses allowed for through the equivalent thickness t_{eq}.

$$\sigma_{cr} = \frac{k_{cr0}\pi^2E}{12(1-\nu^2)}\left(\frac{t_{eq}}{b}\right)^2 \tag{47}$$

where

$$k_{cr0} = \frac{\sqrt{3A_2 + 6\chi(1 + A_5^{\,2})}}{\pi^2\sqrt{A_1}} + \frac{2(1-\nu)A_3 - 2A_4}{\pi^2A_1} + \frac{3A_2 + 6\chi(1 + A_5^{\,2})}{\pi^2\sqrt{A_1[3A_2 + 6\chi(1 + A_5^{\,2})]}}$$

and t_{eq} can be determined from Eqs (42)-(44):

$$t_{eq} = \begin{cases} \left(-3.06e^{\frac{-m}{3.7}} + 4.06\right)t & (m \geq 0) \\ \left(0.8e^{\frac{m}{0.7}} + 0.22\right)t & (m < 0) \end{cases}$$ for simply-supported edges

$$t_{eq} = \begin{cases} \left(-3e^{\frac{-m}{4.6}} + 4\right)t & (m \geq 0) \\ \left(0.75e^{m} + 0.25\right)t & (m < 0) \end{cases}$$ for elastically restrained edges

$$t_{eq} = \begin{cases} \left(-3.2e^{\frac{-m}{6.4}} + 4.2\right)t & (m \geq 0) \\ \left(0.7e^{\frac{m}{1.3}} + 0.3\right)t & (m < 0) \end{cases}$$ for clamped edges

7. Conclusions

A new model for calculating the elastic local buckling stress of steel plates in square CFST columns has been proposed, in which the influence of tensile hoop stresses in the steel plate is considered. The calculated results from the proposed model have been compared with both experimental results and those from previous models. The proposed model provides better agreement with the experiments in comparison with previous models due to the allowance made for the influence of the tensile hoop stresses that arise due to the presence of the concrete infill. The proposed model also has broader applicability than steel plates in square CFST sections, and can be used to assess the influence of hoop stresses (tensile or compressive), boundary conditions and width-to-wall thickness (b/t) ratios on the critical local buckling stress of steel plates. Based on the results and analysis presented in this paper, the follow conclusions may be drawn:

(1) Tensile hoop stresses that arise in the steel plates of CFST columns under axial compression delay the occurrence of local buckling.

(2) The elastic critical local buckling stress σ_{cr} of steel plates in square CFST columns is influenced principally by the b/t ratio, the level of tensile hoop stresses and the restraining factor along the unloaded edges χ. The critical stress σ_{cr} increases with decreasing b/t ratios, increasing tensile hoop stresses and increasing values of χ. Of these parameters, the b/t ratio has the most influence, followed by the tensile hoop stresses and finally χ.

(3) The influence of the tensile hoop stresses on the elastic critical local buckling stress σ_{cr} reduces with increasing rotational edge restraint, while the influence of χ on σ_{cr} reduces with increasing tensile hoop stresses.

(4) A parameter δ_m has been introduced to reflect the influence of the ratio of the tensile hoop stress to the axial

compressive stress m on the elastic critical local buckling stress. The relationship between δ_m and m for a given value of χ is essentially linear and can be formulated as a linear equation.

(5) As an alternative to the primary model presented, a model in which the influence of the tensile hoop stresses in the steel plates of CFST sections is captured using an equivalent thickness concept, has also been proposed, and sufficiently straightforward for application in engineering design practice.

Acknowledgments

The authors would like to thank Miss Pui Yee Chung for her assistance. This research was funded by the National Natural Sciences Foundation of China (Grant No. 51008085 and Grant No. 11472084), Guangzhou Pearl River New Star of Science & Technology Project (Grant No. 2012J2200100), China Scholarship Council (Grant No. 201608440006) and China Postdoctoral Science Foundation (Grant No. 2012M511810 and No. 2014T70807).

References

[1] K. Sakino, H. Nakahara, S. Morino, I. Nishiyama, Behaviour of centrally loaded concrete-filled steel-tube short columns, J. Struct. Eng. ASCE 130 (2) (2004) 180-188.

[2] D. Liu, W. M. Gho, Axial load behavior of high-strength rectangular concrete-filled steel tubular stub columns, Thin-Walled Struct. 43 (8) (2005) 1131-1142.

[3] F. Abed, M. AlHamaydeh, S. Abdalla, Experimental and numerical investigations of the compressive behavior of concrete filled steel tubes (CFSTs), J. Constr. Steel Res. 80 (2013) 429-439.

[4] A. K. H. Kwan, C. X. Dong, J. C. M. Ho. Axial and lateral stress–strain model for circular concrete-filled steel tubes

with external steel confinement, Eng. Struct. 117(2016) 528-541.

[5] Z.-L. Zuo, J. Cai, C. Yang, Q.-J. Chen, G. Sun, Axial load behavior of L-shaped CFT stub columns with binding bars, Eng. Struct. 37 (2012) 88-98.

[6] M.H. Lai, J.C.M. Ho, An analysis-based model for axially loaded circular CFST columns, Thin-Walled Struct.119 (2017) 770-781.

[7] H. B. Ge, T. Usami, Strength of concrete-filled thin-walled steel box column: experiment, J. Struct. Eng. ASCE 118 (11) (1992) 3036-3054.

[8] H. B. Ge, T. Usami, Strength analysis of concrete-filled thin-walled steel box column, J. Constr. Steel Res. 30 (1994) 259-281.

[9] H. D. Wright, Buckling of steel plates in contact with a rigid medium, Struct. Eng. 71 (12) (1993) 209-215.

[10] H. D. Wright, Local stability of filled and encased steel sections, J. Struct. Eng. ASCE 121 (10) (1995) 1382-1388.

[11] M. A. Bradford, H.Y. Loh, B. Uy, Slenderness limits for filled circular steel tubes, J. Constr. Steel Res. 58 (2002) 234-252.

[12] B. Uy, M. A. Bradford, Elastic local buckling of steel plates in composite steel-concrete members, Eng. Struct. 18 (3) (1996) 193-200.

[13] B. Uy, Local and post-local buckling of concrete filled steel welded box columns, J. Constr. Steel Res. 47 (1998) 47-72.

[14] B. Uy, Local and post-local buckling of fabricated steel and composite cross sections, J. Struct. Eng. ASCE 127(6) (2001) 666-677.

[15] D. Li, Z. Huang, B. Uy , H-T Thai , C. Hou, Slenderness limits for fabricated S960 ultra-high-strength steel and composite columns, J. Constr. Steel Res. 159 (2019) 109-121.

[16] Q. Q. Liang, B. Uy, Theoretical study on the post-local buckling of steel plates in concrete-filled box columns,

Comput. Struct. 75 (5) (2000) 479-490.

[17] Q. Q. Liang, B. Uy, J. Y. R. Liew, Nonlinear analysis of concrete-filled thin-walled steel box columns with local buckling effects, J. Constr. Steel Res. 62 (2006) 581-591.

[18] Q. Q. Liang, B. Uy, J. Y. R. Liew, Local buckling of steel plates in concrete-filled thin walled steel tubular beam-columns, J. Constr. Steel Res. 63(3) (2007) 396-405.

[19] G. M. Kamil, Q. Q. Liang, M. N.S. Hadi, Local buckling of steel plates in concrete-filled steel tubular columns at elevated temperatures, Eng. Struct.168 (2018) 108-118.

[20] J. Cai, Y.-L. Long, Local buckling of steel plates in rectangular CFT stub columns with binding bars, J. Constr. Steel Res. 65 (4) (2009) 965-972.

[21] Y.-L. Long, J. Wan, J. Cai. Theoretical study on local buckling of rectangular CFT columns under eccentric compression, J. Constr. Steel Res. 120 (2016) 70-80.

[22] Y.-L. Long, L. Zeng, A refined model for local buckling of rectangular CFST columns with binding bars, Thin-Walled Struct. 132 (2018) 431-441.

[23] S.T. Smith, M.A. Bradford, D.J. Oehlers, Numerical convergence of simple and orthogonal polynomials for the unilateral plate buckling problem using the Rayleigh-Ritz method, Int J Numer. Meth. Eng. 44 (1999) 1685-1707.

[24] S. P. Timoshenko, J. M. Gere. Theory of Elastic Stability, second ed. McGraw-Hill, New York, 1961.

[25] J.P. Mander, M.J.N Priestley, R.Park, Theoretical stress-strain model for confined concrete, J. Struct. Eng. ASCE 114(8) (1988)1807-1826

[26] Y.S. Huang, Y.-L. Long, J. Cai, Ultimate strength of rectangular concrete-filled steel tubular (CFT) stub columns under axial compression, Steel Compos. Struct. 8(2) (2008) 115-128.

[27] Y.-L. Long, J Cai, Stress-strain relationship of concrete confined by rectangular steel tubes with binding bars, J. Constr. Steel Res. 88 (2013) 1-14.

Appendix

$$A_1 = \frac{1}{3} + \frac{\phi_1}{2} + \frac{\phi_1^2 + 2\phi_2}{5} + \frac{\phi_3 + \phi_1\phi_2}{3} + \frac{\phi_2^2 + 2\phi_1\phi_3}{7} + \frac{\phi_2\phi_3}{4} + \frac{\phi_3^2}{9}$$

$$A_2 = 4\phi_1^2 + 12\phi_2^2 + 12\phi_1\phi_2 + \frac{144}{5}\phi_3^2 + 16\phi_1\phi_3 + 36\phi_2\phi_3$$

$$A_3 = 1 + 3\phi_1 + 2\phi_1^2 + 4\phi_2 + 5\phi_3 + 5\phi_1\phi_2 + 6\phi_1\phi_3 + 7\phi_2\phi_3 + 3\phi_2^2 + 4\phi_3^2$$

$$A_4 = \phi_1 + \frac{2\phi_1^2 + 6\phi_2}{3} + 3\phi_3 + 2\phi_1\phi_2 + \frac{14\phi_1\phi_3 + 6\phi_2^2}{5} + 3\phi_2\phi_3 + \frac{12\phi_3^2}{7}$$

$$A_5 = 1 + 2\phi_1 + 3\phi_2 + 4\phi_3$$

$$\phi_1 = \chi$$

$$\phi_2 = -2(\chi + 1)$$

$$\phi_3 = \chi + 1$$

Nomenclature

a	local buckling half-wavelength
b	width of steel plate
t	thickness of steel plate
v	Poisson's ratio of the steel plate
χ	elastic restraining factor on unloaded edges
γ	half-wave parameter
ζ_r	rotational rigidity of elastic restraint on unloaded edges
D	flexural rigidity of steel plate
E	elastic modulus of steel plate
Π	total potential energy of steel plate
U	energy associated with thin plate bending
U_Γ	energy associated with elastic restraint along unloaded edges
V	work done by applied loading
ω	deflection function
σ_x	uniform compressive hoop stress in the x-direction
σ_y	uniform tensile hoop stress in the y-direction
m	ratio of tensile hoop stress to longitudinal compressive stress, taken as $m=-\sigma_y/\sigma_x$
N_x	normal force per unit length in the x-direction
N_y	normal force per unit length in the y-direction
τ_{xy}	shear stress acting in cross-sections perpendicular to the x-axis and in the direction of the y-axis
k_{cr}	critical buckling coefficient which considers the influence of the hoop stress
k_{cr0}	critical buckling coefficient which neglects the influence of the hoop stress
f_y	yield strength of steel plate
$\sigma_{cr,test}$	elastic critical local buckling stress measured in experiment
σ_{cr}	calculated elastic critical local buckling stress of steel plate
σ_{cr1}	calculated elastic critical local buckling stress of steel plate when $m>0$
σ_{cr0}	calculated elastic critical local buckling stress of steel plate when $m=0$

Figures: Fig. 1-Fig. 13

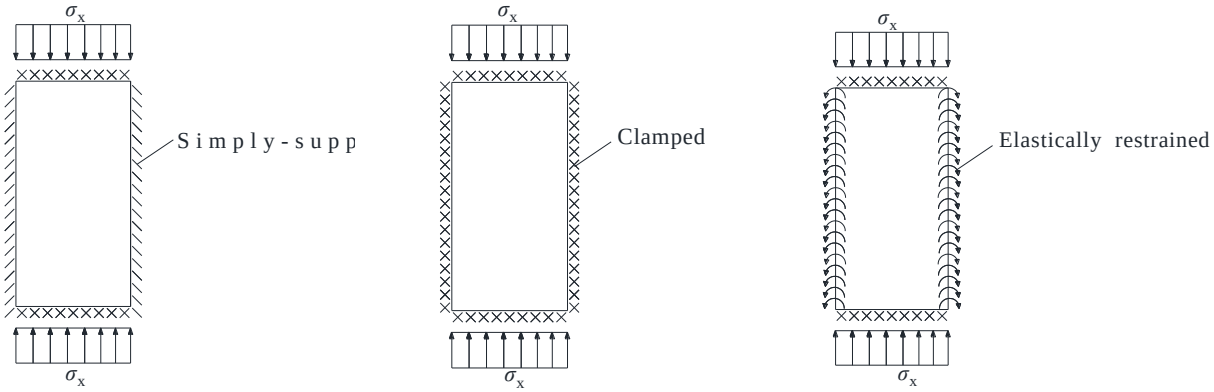

(a) Model proposed in Refs. [9-10] (b) Model proposed in Refs. [16-18] (c) Model proposed in Refs. [20-22]

Fig. 1. Existing models for calculating the elastic local buckling stress of steel plates in square CFST columns

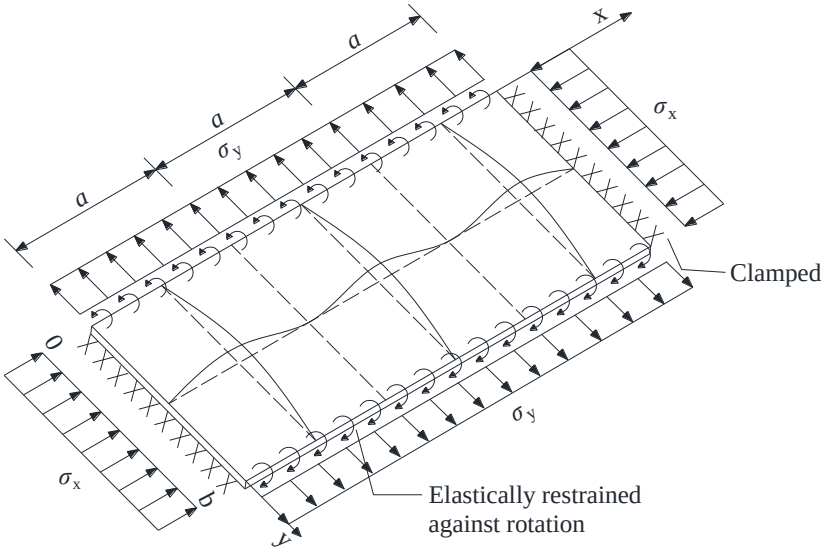

Fig. 2. Local buckling model of steel plate in CFST columns proposed in current study

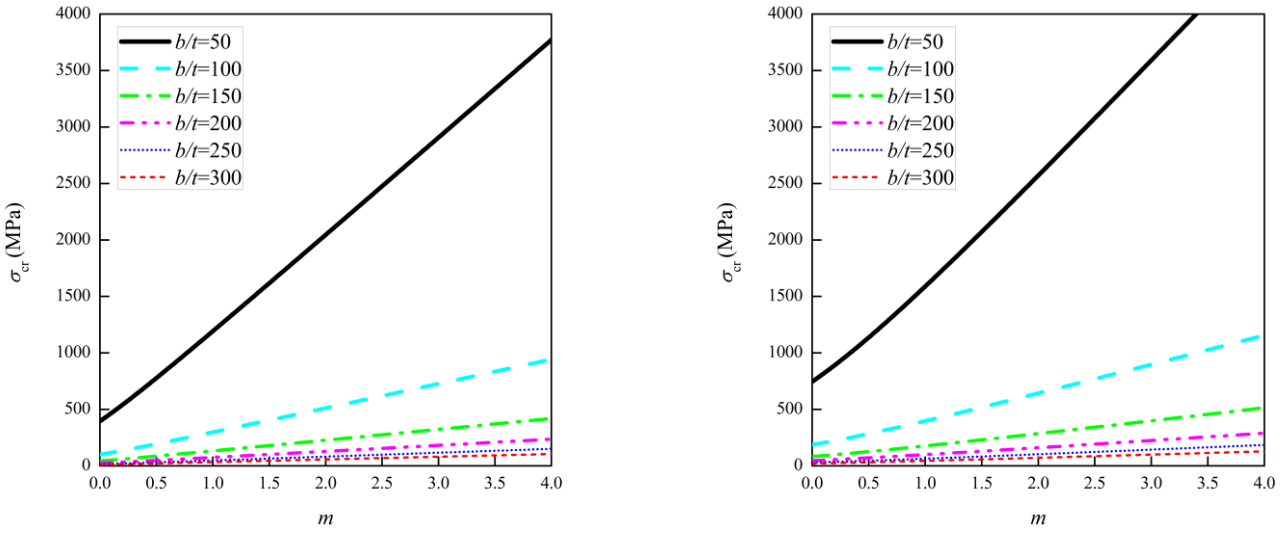

(a) Simply-supported unloaded edges (b) Clamped unloaded edges

Fig. 3 Influence of *m* and *b/t* ratio on σ_{cr} for different boundary conditions

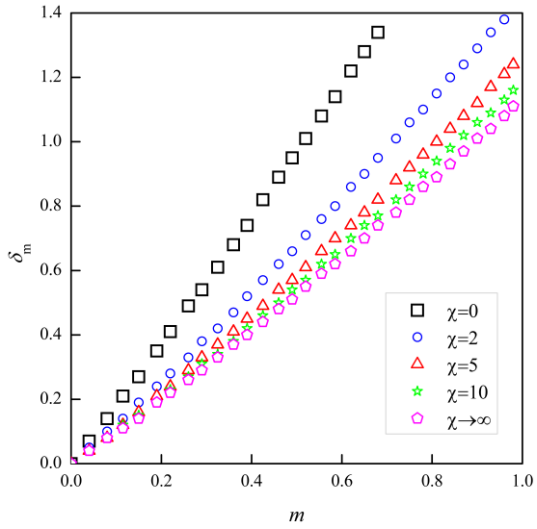

Fig. 4 Relationship between δ_m and m for various values of χ

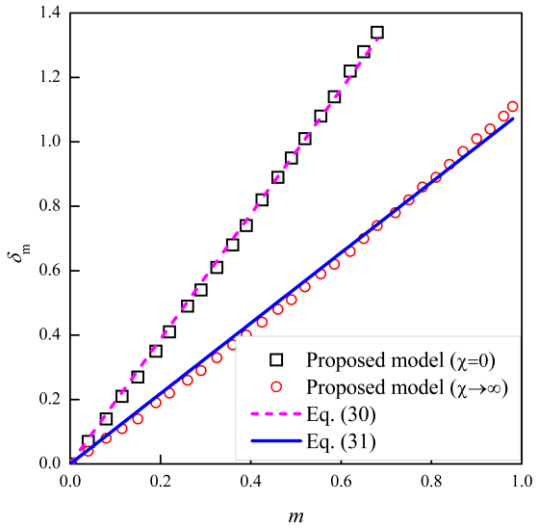

Fig. 5 Comparison between calculated results using the proposed model and those from Eq. (30) and (31) for different boundary conditions

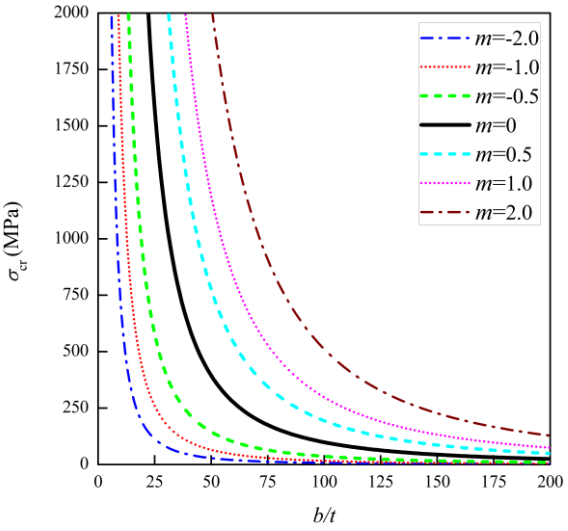

(a) Simply-supported unloaded edges

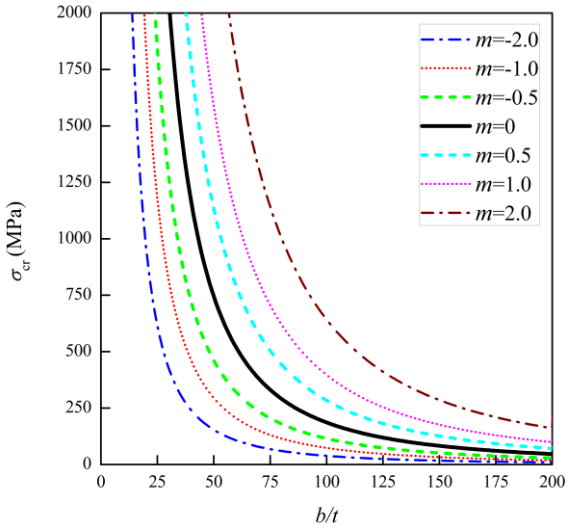

(b) Clamped unloaded edges

Fig. 6 Influence of m on σ_{cr}-b/t curves

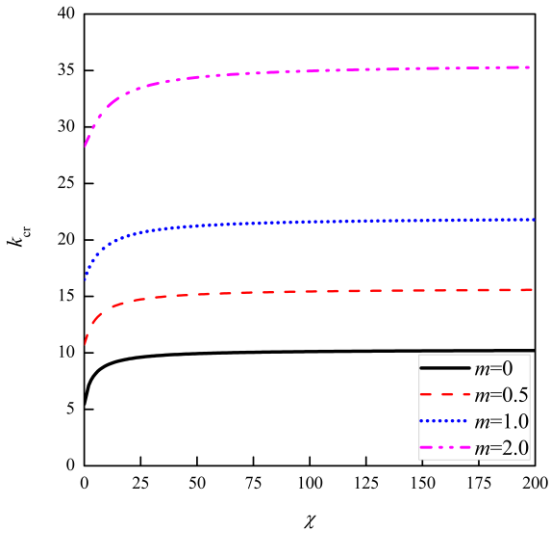

Fig. 7. Influence of χ on k_{cr}

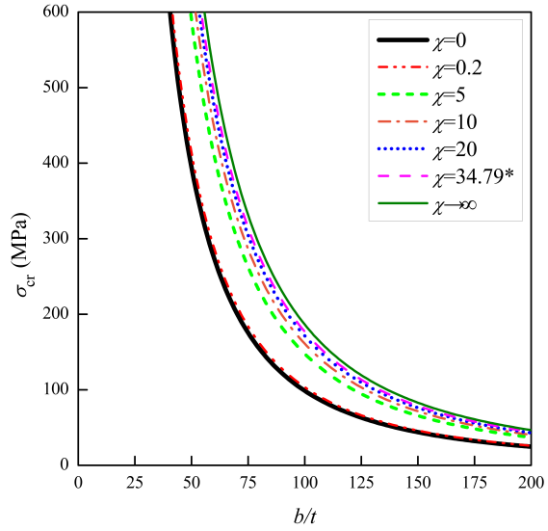

(a) m=0

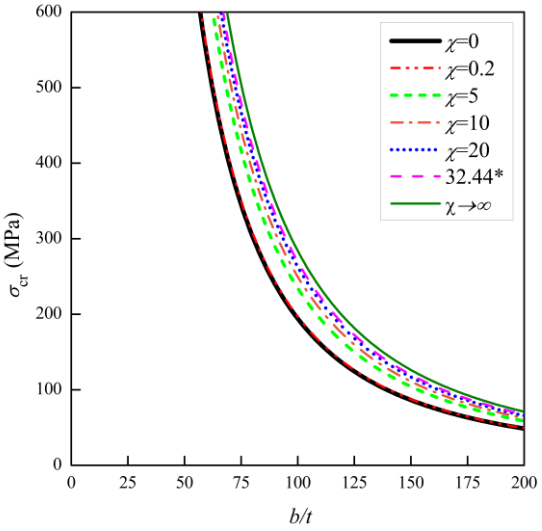

(b) m=0.5

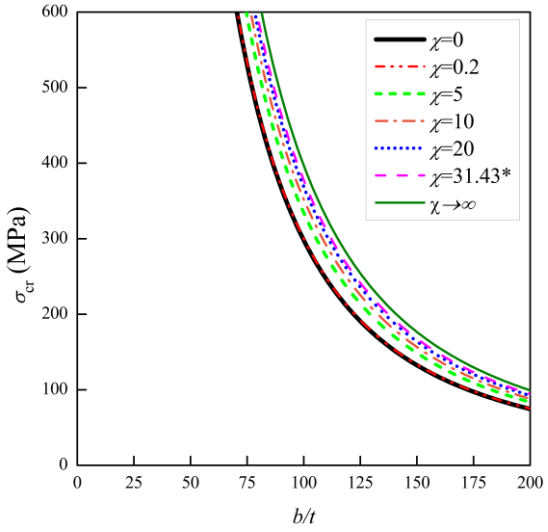

(c) m=1.0

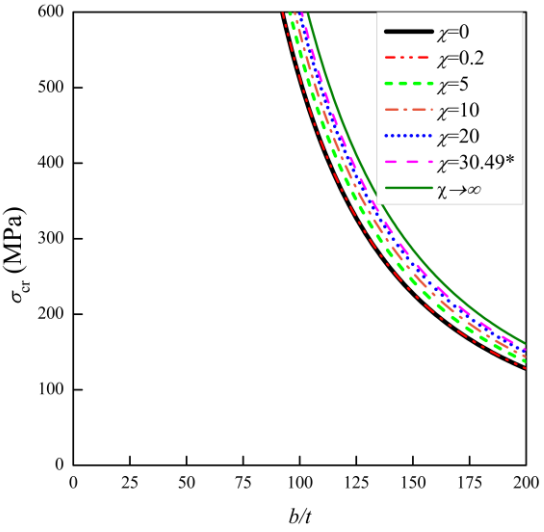

(d) m=2.0

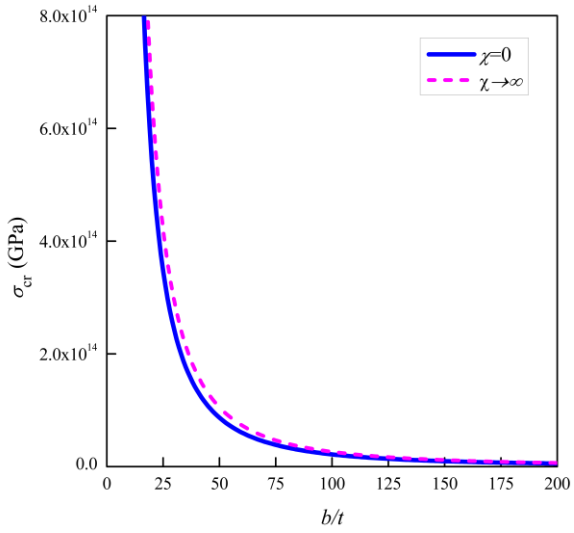

(e) $m \to \infty$

Fig. 8. Influence of χ on σ_{cr}

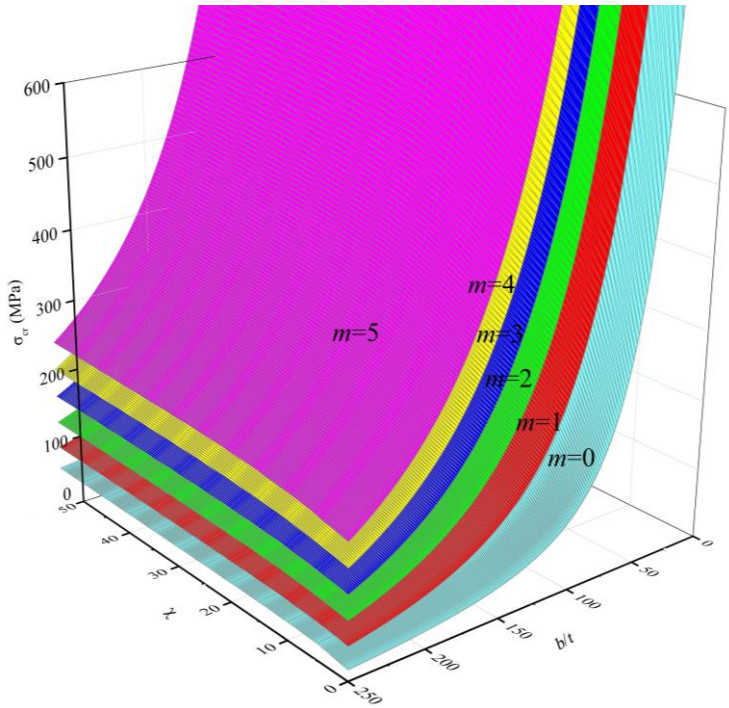

Fig. 9. Influence of b/t ratios, m and χ on σ_{cr}

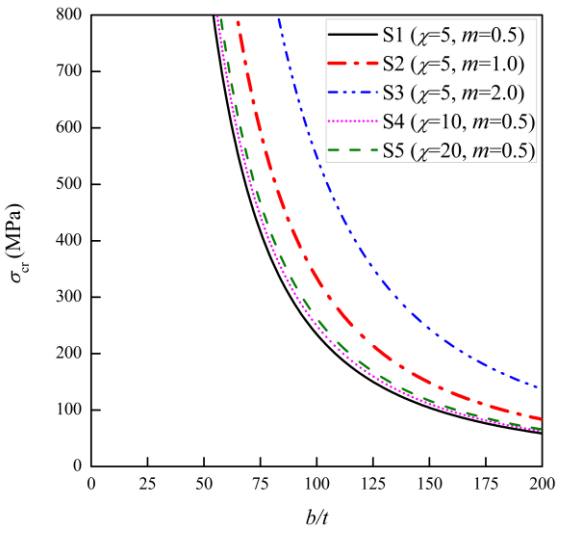

Fig. 10. Influence of χ and m on σ_{cr}

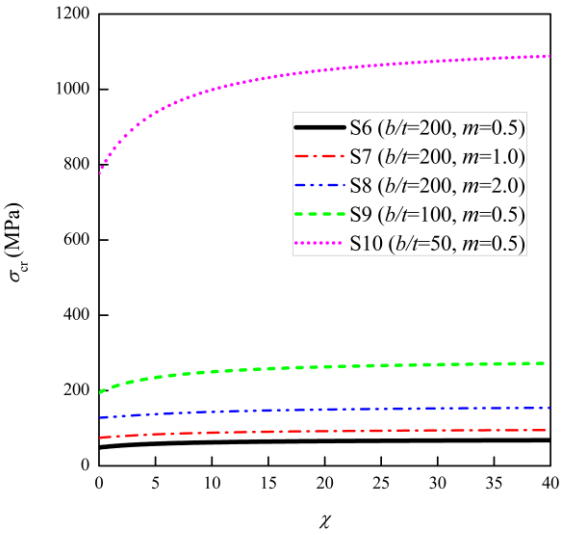

Fig. 11. Influence of b/t and m on σ_{cr}

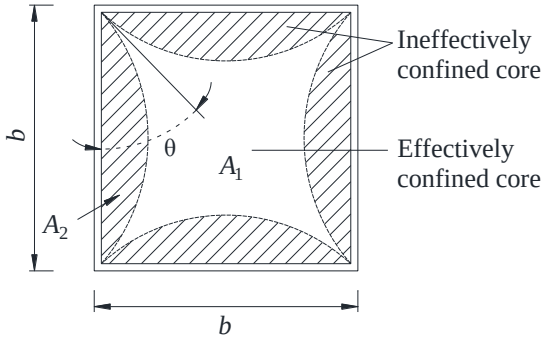

Fig. 12. Effectively confined regions and ineffectively confined regions of concrete core in a CFST section

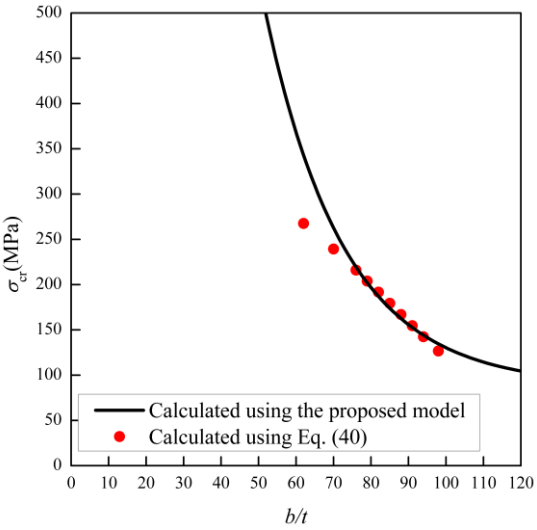

Fig. 13. Comparison of elastic critical local buckling stresses calculated using the proposed model with those from Ref. [17]

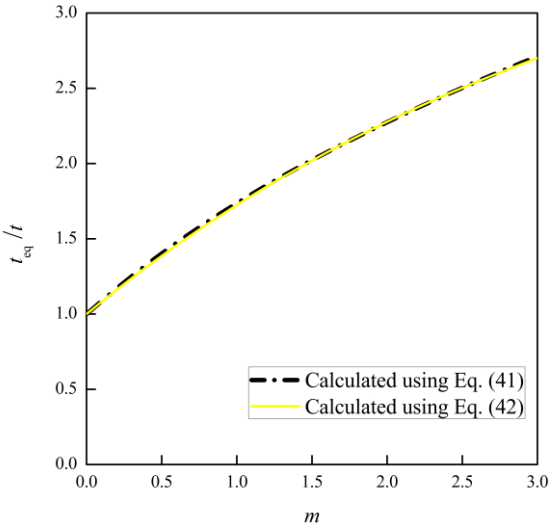

(a) $m \geq 0$, $\chi = 0$

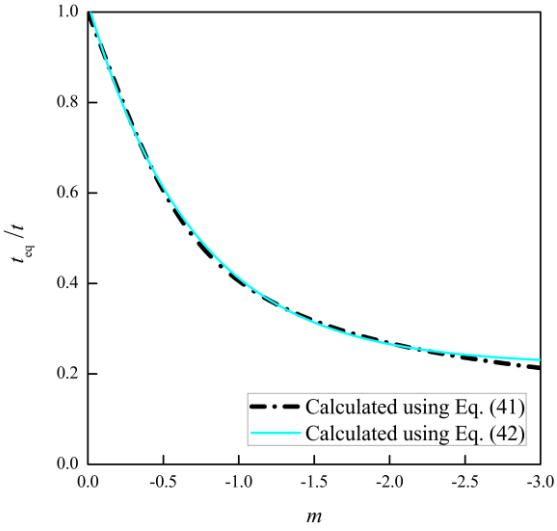

(b) $m < 0$, $\chi = 0$

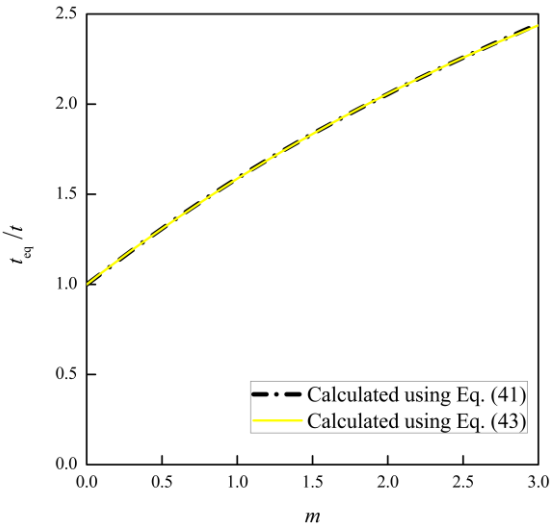

(c) $m \geq 0$, $\chi = 1.46$

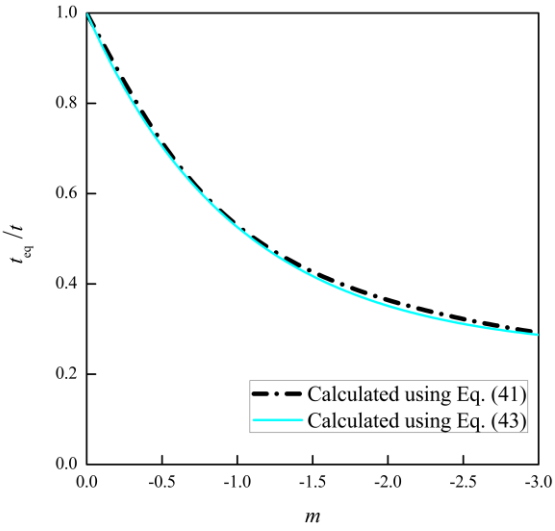

(d) $m < 0$, $\chi = 1.46$

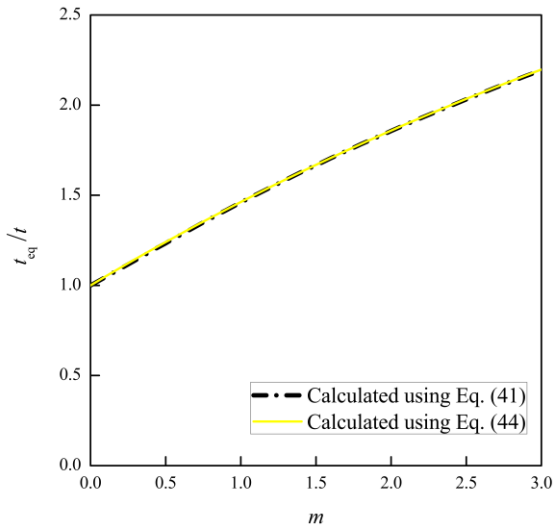

(e) $m \geq 0$, $\chi \to \infty$

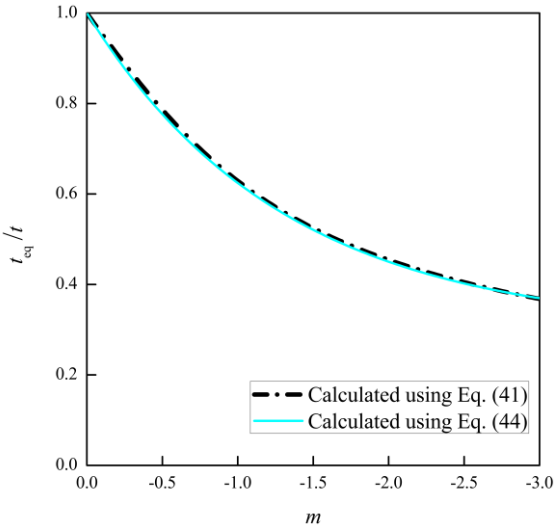

(f) $m < 0$, $\chi \to \infty$

Fig. 14. Relationship between m and t_{eq}/t

Tables: Table 1 – Table 3

Table 1. Relationship between δ_m *and m*

δ_m	Simply-supported unloaded edges (χ=0)	Elastically restrained against rotation (i.e. χ=1.46 for square CFST columns)	Clamped unloaded edges ($\chi\rightarrow\infty$)
5%	*m*=0.03	*m*=0.04	*m*=0.055
10%	*m*=0.055	*m*=0.08	*m*=0.11
15%	*m*=0.085	*m*=0.115	*m*=0.16
20%	*m*=0.11	*m*=0.15	*m*=0.2
25%	*m*=0.14	*m*=0.19	*m*=0.25
30%	*m*=0.165	*m*=0.22	*m*=0.295
35%	*m*=0.19	*m*=0.26	*m*=0.345
40%	*m*=0.215	*m*=0.29	*m*=0.39
45%	*m*=0.245	*m*=0.325	*m*=0.435
50%	*m*=0.27	*m*=0.36	*m*=0.48
55%	*m*=0.295	*m*=0.39	*m*=0.52
60%	*m*=0.32	*m*=0.425	*m*=0.57
65%	*m*=0.345	*m*=0.46	*m*=0.61
70%	*m*=0.37	*m*=0.49	*m*=0.65
75%	*m*=0.395	*m*=0.52	*m*=0.69
80%	*m*=0.42	*m*=0.555	*m*=0.73
85%	*m*=0.445	*m*=0.585	*m*=0.775
90%	*m*=0.47	*m*=0.62	*m*=0.815
95%	*m*=0.49	*m*=0.65	*m*=0.855
100%	*m*=0.65	*m*=0.68	*m*=0.895

Table 2. k_{cr} for different boundary conditions corresponding to various *m*

Boundary conditions	*m*=0	*m*=1	*m*=2	*m*=3	*m*=4	*m*=5	*m*=6	*m*=7	*m*=8
χ=0 (Simply-supported unloaded edges)	5.46	16.49	28.29	34.24	52.16	64.13	76.12	88.10	100.09
χ=0.2	5.73	16.60	28.35	40.25	52.19	64.16	76.13	88.12	100.10
χ=35	9.79	20.97	33.96	47.46	61.14	74.91	88.72	102.56	116.43
$\chi\rightarrow\infty$ (Clamped unloaded edges)	10.31	21.97	35.55	49.65	63.96	78.35	92.80	107.27	121.77

Table 3

Comparison of test results with the calculated results using the models from Refs. [9-10], Refs. [16-18], Ref. [20], i.e. Eq. (28) and the proposed model i.e. Eq. (26) for the elastic critical local buckling stress of steel plates in square CFST columns under axial compression.

Source	Specimen no.	b (mm)	t (mm)	b/t	E (MPa)	f_y (MPa)	$\sigma_{cr,test}$ (MPa)	Model from [9-10]		Model from [16-18]		Model from [20]		Proposed model	
								σ_{cr} (MPa)	$\sigma_{cr}/\sigma_{cr,test}$	σ_{cr} (MPa)	$\sigma_{cr}/\sigma_{cr,test}$	σ_{cr} (MPa)	$\sigma_{cr}/\sigma_{cr,test}$	σ_{cr} (MPa)	$\sigma_{cr}/\sigma_{cr,test}$
Ref.[13]	LB1	120	3	40	200000	300	300.0	300.0	1.00	300.0	1.00	300.0	1.00	300.0	1.00
	LB3	150	3	50	200000	300	300.0	300.0	1.00	300.0	1.00	300.0	1.00	300.0	1.00
	LB5	180	3	60	200000	300	300.0	274.2	0.91	300.0	1.00	300.0	1.00	300.0	1.00
	LB7	240	3	80	200000	300	200.0	154.2	0.77	291.2	1.46	192.8	0.96	198.1	0.99
	LB9	300	3	100	200000	300	120.0	98.7	0.82	186.4	1.55	123.4	1.03	123.7	1.03
Ref.[14]	FB1	360	3	120	200000	265	93.4	68.5	0.73	129.4	1.39	85.7	0.92	95.3	1.02
	FB2	420	3	140	200000	265	79.9	50.4	0.63	95.1	1.19	63.0	0.79	70.9	0.89
	FB3	480	3	160	200000	265	43.7	38.6	0.88	72.8	1.67	48.2	1.10	48.5	1.11
	FB4	540	3	180	200000	265	38.8	30.5	0.79	57.5	1.48	38.1	0.98	38.6	0.99
	Mean								0.84		1.30		0.98		1.00
	COV								0.12		0.25		0.08		0.05